EPJ Web of Conferences **259**, 01006 (2022) https://doi.org/10.1051/epjconf/202225901006
SQM 2021

Updates on Flavor Production from STAR

Sooraj Radhakrishnan[1,*]

[1]Kent State University, Kent, OH, 44240

Abstract. In these proceedings, some of the latest results from the STAR experiment on heavy, strange and light flavor hadron production and their flow are summarized. Over the years STAR has collected heavy ion collision data over a wide range of collision energies from $\sqrt{s_{\rm NN}}$ = 200 GeV down to $\sqrt{s_{\rm NN}}$ = 3 GeV. In high energy heavy ion collisions, heavy flavor hadrons are a valuable probe to study properties of the Quark Gluon Plasma (QGP) created in these collisions. Measurements of strange and light flavor hadrons at lower collision energies help understand the properties of the QCD matter at finite baryon densities and the phase structure of the QCD matter. Furthermore, the high statistics data collected at $\sqrt{s_{\rm NN}}$ = 3 GeV allows measurements of hypernuclei production and flow, which can provide insights into the hyperon - nucleon interactions and hyperon contribution to the nuclear equation of state.

1 Introduction

Measurements of elliptic flow (v_2) of D mesons and electrons from heavy flavor hadron decays (HFE) in heavy-ion collisions at top RHIC energy and LHC energies show comparable values to those of light flavor hadrons, indicating that charm quarks interact strongly with the Quark Gluon Plasma (QGP) at these energies [1, 2]. These measurements have helped constrain the charm quark diffusion coefficient in the QGP [3]. Measurements of HFE v_2 at lower collision energies can help constrain the temperature dependence of charm quark transport in the QGP. The observed J/ψ nuclear modification factor (R_{AA}) in heavy-ion collisions at RHIC and LHC has contributions from a regeneration component, in addition to that from in-medium dissociation [4]. Better precision measurements at lower collision energies can also help constrain these different contributions.

The Beam Energy Scan Phase II (BES-II) program at STAR, following the BES-I, aims to conduct high statistics measurements of various observables in the high baryon density region ($200 < \mu_B < 720$ MeV) to understand the phase structure of QCD matter. As part of BES-II, STAR has collected a high statistics dataset of Au+Au collisions at $\sqrt{s_{\rm NN}}$ = 3 GeV (μ_B = 720 MeV), using a fixed-target setup. The detailed measurements of the collective flow of various identified light and strange flavor hadrons with this dataset can improve our understanding of the nature and Equation of State (EoS) of the QCD matter in the high μ_B region. In addition, the high statistics 3 GeV dataset allows the measurement of strange and multi-strange hadron production, providing insights into the canonical suppression of strangeness production at low collision energies [6]. The same dataset also enables measurements of the yields, lifetime and flow of hypernuclei, owing to their enhanced cross-sections at these low energies, which can

*e-mail: skradhakrishnan@lbl.gov

help understand the hyperon - nucleon interactions and hyperon contribution to the nuclear EoS.

In these proceedings, measurements of HFE v_2 in Au+Au collisions at $\sqrt{s_{\rm NN}}$ = 54.4 and 27 GeV and R_{AA} of J/ψ in Au+Au collisions at $\sqrt{s_{\rm NN}}$ = 54.4 GeV are presented. Measurements of v_2 of identified hadrons, yield ratios of strange and multi-strange hadrons, and yields, lifetime and directed flow (v_1) of hypernuclei ${}^{\Lambda}_{3}H$ and ${}^{\Lambda}_{4}H$ in Au+Au collisions at $\sqrt{s_{\rm NN}}$ = 3 GeV are also presented. The results are compared to model calculations and the physics implications are discussed.

2 Heavy flavor measurements at $\sqrt{s_{\rm NN}}$ = 54.4 and 27 GeV

STAR had previously carried out measurements of v_2 of HFE at $\sqrt{s_{\rm NN}}$ = 62.4 and 39 GeV [2]. The measured HFE v_2 values were found to be smaller, although consistent within the large uncertainties, than the values measured at 200 GeV. In 2017 and 2018 STAR collected 10 times more statistics at $\sqrt{s_{\rm NN}}$ = 54.4 GeV and 27 GeV compared to those used for previous measurements at 62.4 and 39 GeV. The left panel of Fig. 1 shows the measured v_2 of HFE at 54.4 and 27 GeV as a function of transverse momentum ($p_{\rm T}$), compared to the measurements at 200 GeV. The measured v_2 values at 54.4 GeV are non-zero and comparable to those at 200 GeV, indicating strong interactions of the charm quarks with the QGP medium. The measurements at 27 GeV show a hint of lower values, albeit with large uncertainties. The right panel of Fig. 1 shows the comparison of the measured HFE v_2 values at 54.4 GeV to different theoretical model calculations. The TAMU [7] and PHSD [8] model calculations, which incorporate charm quark diffusion in the QGP, describe the data at high $p_{\rm T}$, but are lower than the measured values at low $p_{\rm T}$.

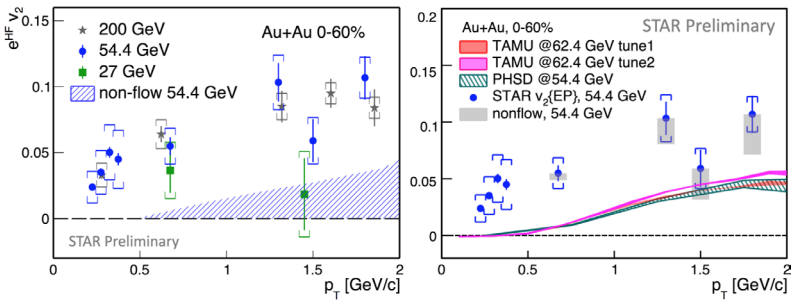

Figure 1. (Left) The v_2 of HFE as a function of $p_{\rm T}$ in 0-60% Au+Au collisions compared between $\sqrt{s_{\rm NN}}$ = 54.4, 27 and 200 GeV. The error bars are statistical uncertainties and brackets indicate systematic uncertainties. The blue hatched area indicates the estimated non-flow contribution to the measured v_2 values. (Right) The v_2 of HFE as a function of $p_{\rm T}$ in 0-60% Au+Au collisions at $\sqrt{s_{\rm NN}}$ = 54.4 GeV compared to different model calculations [7, 8].

The in-medium dissociation of J/ψ, due to Debye like color screening in the QGP medium, has been proposed as an evidence of the formation of the QGP and a valuable tool to study its properties, particularly the medium temperature [9]. Suppression of J/ψ production has been observed at both RHIC and the LHC. However, the observed suppression also gets contribution from regeneration of J/ψ from deconfined charm quarks in the medium [4, 10]. Measurements of the J/ψ suppression at a lower collision energy of $\sqrt{s_{\rm NN}}$ = 54.4 GeV, where the charm quark production cross-section and thus the regeneration contribution are lower, can help better understand the in-medium J/ψ dissociation. The left panel of Fig. 2 shows the

nuclear modification factor R_{AA}, the ratio of yields in A+A collisions to that in p+p collisions scaled by the number of binary nucleon-nucleon collisions N_{coll}, as a function of number of participating nucleons in the collision (N_{part}) for different collision energies. The right panel shows the R_{AA} in central collisions as a function of collision energy. The new measurements at 54.4 GeV are shown in red markers, and have significantly improved precision compared to previous low energy STAR measurements at 62.4 and 39 GeV [11]. The measured values show no significant collision energy dependence from 17.2 to 200 GeV within uncertainties. A model calculation [10] that takes into account both in-medium dissociation and regeneration, along with cold nuclear matter effects, can reproduce the measured values.

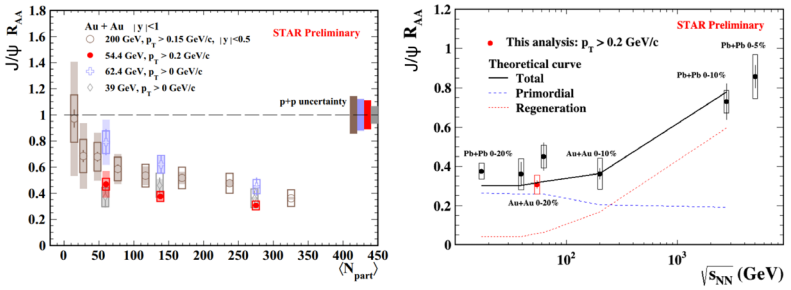

Figure 2. (Left) The R_{AA} of J/ψ as a function of N_{part} for different collision energies. The error bars, boxes and shaded bands on the data points denote statistical, systematic and N_{coll} uncertainties respectively. The shaded bands at 1 indicate the uncertainties from the p+p baseline. (Right) The R_{AA} of J/ψ in central collisions as a function of collision energy, including measurements at SPS and LHC [12]. The error bands indicate statistical uncertainties and boxes indicate the combined systematic, N_{coll} and p+p baseline uncertainties.

3 Strange and light flavor production

3.1 Disappearance of partonic collectivity at $\sqrt{s_{NN}}$ = 3 GeV

The large positive values of v_2 and its number of constituent quark (NCQ) scaling observed for identified hadrons in high energy heavy-ion collisions have been argued as evidence for the creation of a strongly interacting QGP [13]. At lower collision energies, below $\sqrt{s_{NN}}$ = 27 GeV, where the passage time of the colliding nuclei becomes comparable to or larger than the time scale of parton production, a negative 'squeeze out' contribution from the shadowing by spectator nucleons is expected for the v_2, in addition to the contribution from partonic collectivity [14]. At even lower collision energies, $\sqrt{s_{NN}} \sim 5$ GeV, hadronic transport and baryonic mean field interactions among the colliding nuclei also contribute to the observed flow harmonics [15]. In 2018 STAR collected about 2.6×10^8 minimum bias Au+Au collisions at $\sqrt{s_{NN}}$ = 3 GeV. The high statistics dataset allows to carry out detailed measurements of the v_2 of various identified hadrons at mid-rapidity in this interesting region of QCD phase space.

Figure 3 shows the NCQ scaled v_2 of identified hadrons as a function of the scaled transverse kinetic energy in Au+Au collisions at $\sqrt{s_{NN}}$ = 3 GeV. The figure also shows measurements at $\sqrt{s_{NN}}$ = 4.5 GeV [5] and from the new datasets at $\sqrt{s_{NN}}$ = 54.4 and 27 GeV. The v_2 values at 54.4 and 27 show NCQ scaling. Positive values and scaling within uncertainties are also observed at $\sqrt{s_{NN}}$ = 4.5 GeV. At $\sqrt{s_{NN}}$ = 3 GeV, the measured v_2 values turn negative and the NCQ scaling breaks down. Figure 4 shows the centrality dependence of the v_2 values of different identified hadrons at $\sqrt{s_{NN}}$ = 3 GeV. Calculations from the UrQMD model [16]

at $\sqrt{s_{\rm NN}}$ = 3 GeV in the cascade mode, that incorporates hadronic transport and spectator shadowing, and in the meanfield mode, which includes additional baryonic meanfield interactions, are also shown. The UrQMD cascade mode cannot describe the measured v_2 values and are of opposite sign. The UrQMD meanfield mode calculations, with a value of the incompressibility κ = 380 MeV, can reproduce the trends in the data, except for K^+. These measurements and comparisons show that a medium dominated by hadronic and baryonic interactions, rather than partonic interactions, is produced in Au+Au collisions at $\sqrt{s_{\rm NN}}$ = 3 GeV.

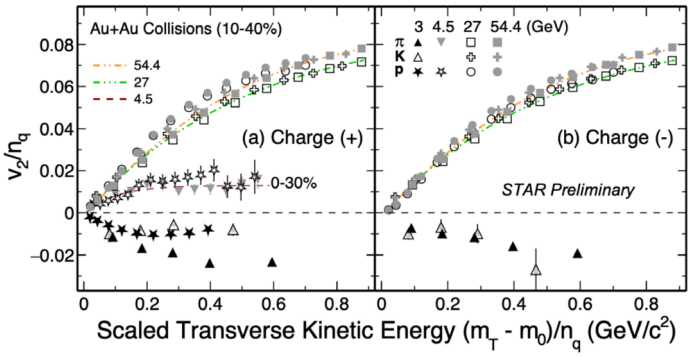

Figure 3. The v_2 scaled by the number of constituent quarks n_q as a function of the scaled transverse kinetic energy at different collision energies for negative (left) and positive particles (right). Statistical and systematic uncertainties are indicated by error bars and shaded bands on data points, respectively. The dashed lines denote the NCQ scaling curves at different energies.

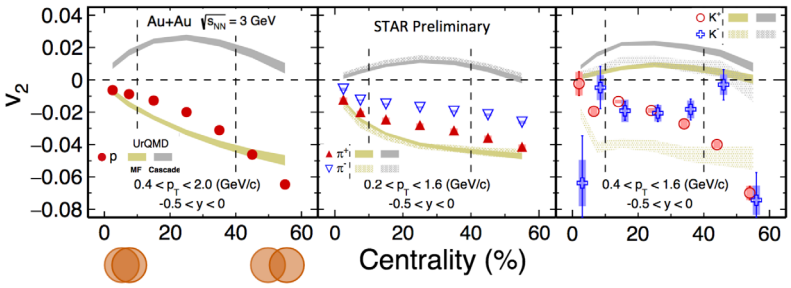

Figure 4. The v_2 of protons (left), pions (middle) and kaons (right) as a function of centrality for Au+Au collisions at $\sqrt{s_{\rm NN}}$ = 3 GeV. Statistical and systematic uncertainties are indicated by error bars and shaded bands on data points, respectively. UrQMD calculations in cascade and meanfiled modes are shown as gray and golden bands respectively.

3.2 Canonical suppression of strangeness production

Statistical thermal models have been successful in describing the hadron yields in heavy-ion collisions [17]. At low collision energies and in small collision systems, as the strangeness production is rare, it has been argued that the strangeness number needs to conserved locally and on an event by event basis. Therefore a Canonical Ensemble (CE) is more suitable to describe the statistical production of strange hadrons as opposed to a Grand Canonical Ensemble (GCE). This would cause progressive suppression of yields of strange hadrons with non-zero strangeness numbers [6, 18]. Figure 5 shows the yield ratios of ϕ mesons to that of K^- on the

left and yield ratios of ϕ relative to Ξ^- on the right as a function of collision energy. The new measurements at 3 GeV are shown as colored markers. The GCE calculations are strongly disfavored, being lower than the measured ratios at 5σ and 4σ significances respectively, in the 0-10% most central collisions. The CE calculation with a strangeness correlation length (r_c) $\sim$ 3.2 fm can describe the ϕ/K^- yield ratio. There is a hint of a centrality dependence of the ratios at $\sqrt{s_{\rm NN}}$ = 3 GeV. Future higher precision measurements can provide better insights into the centrality dependence. Transport model calculations from a modified UrQMD [19] and SMASH [20] that take into account high mass resonances that decay into ϕ and Ξ^- can also describe the ratios at 3 GeV.

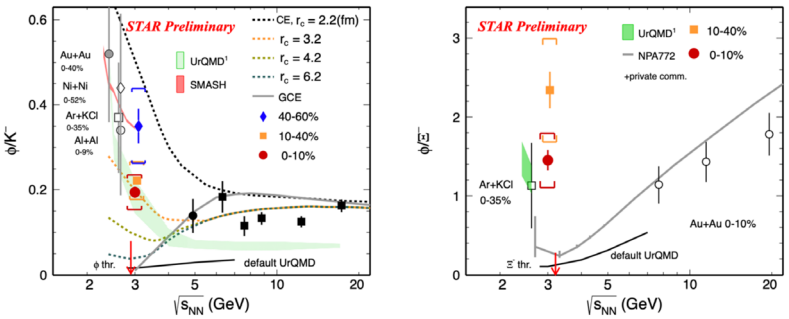

Figure 5. The yield ratios of ϕ to that of K^- (left) and of ϕ to that of Ξ^- (right) as a function of collision energy. The new measurements at 3 GeV are shown in colored markers and at other energies [21] in solid black and open gray markers. The error bars and brackets on the 3 GeV data points denote the statistical and systematic uncertainties respectively. The gray solid line indicates the GCE calculation while the dashed lines indicate CE calculations with different r_c values [6, 18, 22]. The default UrQMD [16] calculations are shown in solid black line, while the modified UrQMD [19] and SMASH [20] calculations are shown in the green and red bands respectively.

4 Hypernuclei production at $\sqrt{s_{\rm NN}}$ = 3 GeV

Hypernuclei production cross-sections in heavy-ion collisions are large at colliding energies $\sim$ 3 GeV [23]. This provides an opportunity to measure the lifetime, yield and collective flow of hypernuclei with the $\sqrt{s_{\rm NN}}$ = 3 GeV Au+Au collision dataset. The lifetimes of ${}^{\Lambda}_{3}H$ and ${}^{\Lambda}_{4}H$ measured using the 3 GeV dataset are 232 $\pm$ 29 (stat) $\pm$ 37 (sys) and 218 $\pm$ 8 (stat) $\pm$ 12 (sys), respectively. The ${}^{\Lambda}_{4}H$ lifetime measurement obtained is the most precise to date. The two left panels of Fig. 6 show the yields within rapidity $|y| < 0.5$ of the hypernuclei ${}^{\Lambda}_{3}H$ and ${}^{\Lambda}_{4}H$, along with model calculations, as a function of collision energy. Thermal model calculations [23] can describe the measured ${}^{\Lambda}_{3}H$ yield at 3 GeV and also at the LHC energy [24]. The thermal model calculations are done with a CE for strangeness production. The model however underpredicts the yield of ${}^{\Lambda}_{4}H$ at 3 GeV. Coalescence model calculations [25] overestimate the ${}^{\Lambda}_{3}H$ yield while under-predict the ${}^{\Lambda}_{4}H$ yield at 3 GeV. A hybrid UrQMD calculation over-predicts yields of both ${}^{\Lambda}_{3}H$ and ${}^{\Lambda}_{4}H$. The right panel of Fig. 6 shows the slope of directed flow at midrapidty, $dv_1/dy|_{y=0}$, of various light nuclei and hypernuclei as a function of their mass for Au+Au collisions at $\sqrt{s_{\rm NN}}$ = 3 GeV. A mass scaling of directed flow slope has been observed for light nuclei which is attributed to the coalescence production of light nuclei [26]. The hypernuclei also show a mass scaling of v_1 slope, albeit with large uncertainties, suggesting coalescence production also for hypernuclei. These measurements will help better constrain the hypernucleus production models and also the hyperon contribution to nuclear EoS.

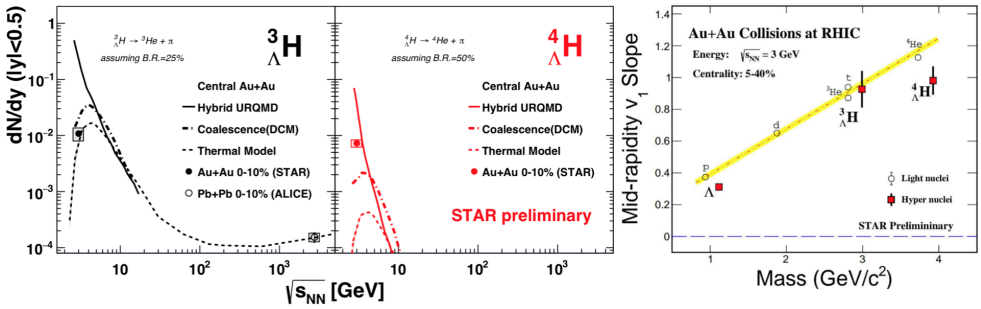

Figure 6. The yield in $|y| < 0.5$ of ${}^{\Lambda}_{3}H$ (left) and ${}^{\Lambda}_{4}H$ (middle), along with model comparisons, as a function of collision energy. The boxes indicate the total uncertainties. (Right) The measured slope, $dv_1/dy|_{y=0}$, in Au+Au collisions at $\sqrt{s_{\rm NN}}$ = 3 of different light nuclei and hypernuclei as a function of mass. Error bars indicate total uncertainties. The yellow line shows a linear fit to the light nuclei measurements. Combined results from the 2-body and 3-body decay channels are used for the ${}^{\Lambda}_{3}H$ v_1 measurements, while for ${}^{\Lambda}_{4}H$ v_1 measurements and for yield measurements of both the hypernuclei results from only 2-body decay channel are used.

5 Summary

We have presented some of the newest measurements from STAR on heavy, strange and light flavor hadron production and collective flow. Measurement of HFE v_2 with a much improved precision in Au+Au collisions at $\sqrt{s_{\rm NN}}$ = 54.4 GeV, compared to previous measurements at 62.4 and 39 GeV, shows non-zero values comparable to the v_2 of HFE measured at 200 GeV. This indicates that charm quarks interact strongly with the QGP medium produced in 54.4 GeV collisions. The R_{AA} of J/ψ measured in Au+Au collisions at $\sqrt{s_{\rm NN}}$ = 54.4 GeV has improved precision compared to previous measurements at 62.4 and 39 GeV. The measurements show no significant collision energy dependence of R_{AA} within uncertainties compared to that at 200 GeV and other lower energy measurements. Elliptic flows of identified hadrons in Au+Au collisions at $\sqrt{s_{\rm NN}}$ = 3 GeV show negative values and a breakdown of the NCQ scaling. Hadronic transport model calculations from UrQMD with baryonic meanfield interactions can describe the trends seen in data. These observations indicate the formation of a medium dominated by hadronic interactions and a nuclear EoS in Au+Au collisions at 3 GeV. Strange and multi-strange hadron yield measurements in Au+Au collisions at $\sqrt{s_{\rm NN}}$ = 3 GeV strongly disfavor GCE calculations and show evidence of canonical suppression in strangeness production. Thermal model calculations are consistent with the measured ${}^{\Lambda}_{3}H$ yield, while under-predct the ${}^{\Lambda}_{4}H$ yield. Coalescence model calculations fail to describe yields of both the hypernuclei. Measurements of directed flow slope, $dv_1/dy|_{y=0}$, of light nuclei and hypernuclei show mass scaling within uncertainties. The mass scaling is consistent with a picture of coalescence production for the light nuclei and hypernuclei.

References

[1] L. Adamczyk et al. (STAR), Phys. Rev. Lett. **118**, 212301 (2017); S. Acharya et al. (ALICE), Phys. Rev. Lett. **120**, 102301 (2018)
[2] L. Adamczyk et al. (STAR), Phys. Rev. C **95**, 034907 (2017)
[3] X. Dong, Y.-J. Lee, R. Rapp, Ann. Rev. Nucl. Part. Sci. **69** 417–445 (2019)

[4] B. Abelev et. al (ALICE), Phys. Lett. B **734**, 314-327 (2014); J. Adam et al. (STAR), Phys. Lett. B **797**, 134917 (2019)
[5] J. Adam et al. (STAR), Phys. Rev. C **103** 34908 (2021)
[6] K. Redlich and A. Tounsi, Eur. Phys. J. C **24**, 589 (2002)
[7] M. He et al., Phys. Rev. C **91**, 024904 (2015)
[8] T. Song et al., Phys. Rev. C **92**, 014910 (2015); T. Song et al., Phys. Rev. C. **96**, 014905 (2017)
[9] T. Matsui, H. Satz, Phys. Lett. B **178** 416–422 (1986).
[10] X. Zhao, R. Rapp, Phys. Rev. C **82**, 064905 (2010)
[11] L. Adamczyk et al. (STAR), Phys. Lett. B **771**, 13 (2017)
[12] L. Kluberg, Eur. Phys. J. C **43**, 145 (2005); B. Abelev et. al (ALICE), Phys. Lett. B **734**, 314 (2014); X. Bai (for ALICE Collaboration), Nucl. Phys. A **1005**, 121769 (2021)
[13] U. Heinz and R. Snellings, Annu. Rev. Nucl. Part. Sci. **63** 123 (2013); B. I. Abelev et al. (STAR), Phys. Rev. Lett. **99**, 112301 (2007)
[14] C. Pinkenburget et al.(E895), Phys. Rev. Lett. **83**, 1295 (1999)
[15] P. Danielewicz et al, Science **298**, 1592-1596, (2002)
[16] M. Bleicheret et al., J. Phys. G **25**, 1859 (1999)
[17] A Andronic et al. Nature **561**, 321 (2018)
[18] A. Andronic et al. Nucl. Phys. A **772** 167-199 (2006)
[19] J. Steinheimer and M. Bleicher, J. Phys. G: Nucl. Part. Phys. **43**, 015104 (2015).
[20] V. Steinberg et al., Phys. Rev. C **99**, 064908 (2019)
[21] M. S. Abdallah et al. (STAR), arXiv:2108.00924 (2021)
[22] S. Wheaton et al., Comput. Phys. Commun. **180**, 84 (2009)
[23] A. Andronic et al., Phys. Lett. B **697**, 203 (2011)
[24] J. Adam et al. (ALICE), Phys. Lett. B **754**, 360 (2016)
[25] J. Steinheimer et al. Phys. Lett. B **714**, 47985 (2012)
[26] L. Adamczyk et al. (STAR), Phys. Rev. C **94**, 034908 (2016)